Current Biology 21, 948–954, June 7, 2011 ©2011 Elsevier Ltd All rights reserved DOI 10.1016/j.cub.2011.04.025

Report

The Arf GAP CNT-2 Regulates the Apoptotic Fate in *C. elegans* Asymmetric Neuroblast Divisions

Aakanksha Singhvi,[1,4] Jerome Teuliere,[1] Karla Talavera,[1] Shaun Cordes,[1,5] Guangshuo Ou,[2,6] Ronald D. Vale,[2] Brinda C. Prasad,[3,7] Scott G. Clark,[3,8] and Gian Garriga[1,*]

[1]Department of Molecular and Cell Biology and Helen Wills Neuroscience Institute, University of California, Berkeley, Berkeley, CA 94720, USA

[2]Howard Hughes Medical Institute and Department of Cellular and Molecular Pharmacology, University of California, San Francisco, San Francisco, CA 94158, USA

[3]Molecular Neurobiology Program and Department of Pharmacology, Skirball Institute of Biomolecular Medicine, NYU School of Medicine, New York, NY 10016, USA

Summary

During development, all cells make the decision to live or die. Although the molecular mechanisms that execute the apoptotic program are well defined, less is known about how cells decide whether to live or die. In *C. elegans*, this decision is linked to how cells divide asymmetrically [1, 2]. Several classes of molecules are known to regulate asymmetric cell divisions in metazoans, yet these molecules do not appear to control *C. elegans* divisions that produce apoptotic cells [3]. We identified CNT-2, an Arf GTPase-activating protein (GAP) of the AGAP family, as a novel regulator of this type of neuroblast division. Loss of CNT-2 alters daughter cell size and causes the apoptotic cell to adopt the fate of its sister cell, resulting in extra neurons. CNT-2's Arf GAP activity is essential for its function in these divisions. The N terminus of CNT-2, which contains a GTPase-like domain that defines the AGAP class of Arf GAPs, negatively regulates CNT-2's function. We provide evidence that CNT-2 regulates receptor-mediated endocytosis and consider the implications of its role in asymmetric cell divisions.

Results and Discussion

Loss of CNT-2 Results in the Production of Extra Neurons

The two *C. elegans* Q.p neuroblasts divide during the first larval stage to produce a posterior daughter (Q.pp) that dies and an anterior daughter (Q.pa) that divides to produce a mechanosensory neuron (AVM on the right; PVM on the left) and an SDQ interneuron [1] (Figure 1A). The Q.p division requires PIG-1, the homolog of the stem cell regulator MELK [4]. *pig-1* mutants produce extra A/PVM and SDQ neurons because Q.pp survives and adopts the fate of its sister (Figure 1B, left). This phenotype differs from that caused by mutations in proapoptotic genes where Q.pp survives but does not divide (Figure 1B, right) [4, 5].

In screens for mutants with extra A/PVMs, we identified the gene *cnt-2*, which encodes an Arf GTPase-activating protein (GAP) of the AGAP (*A*rf GAP with *G* protein-like domain, *A*nkyrin repeat, and *P*H domain) family [6]. *cnt-2* encodes three isoforms (A–C) that contain a G protein-like domain (GLD), a split pleckstrin homology (PH) domain, and two ankyrin repeats (Figures 2A and 2B) [7]. Four mutant alleles exist (Figures 2A and 2B). The *zd168* and *gm390* nonsense mutations were identified in forward genetic screens, whereas the *gm377* and *tm2328* deletions were isolated by reverse genetic approaches.

All *cnt-2* mutants displayed a similar recessive extra A/PVM phenotype (Figure 1C). If *cnt-2* mutations transform the cell fated to die into its sister, these mutations should also produce extra SDQ neurons. Indeed, 52% (n = 150) of *gm377* and 48% (n = 290) of *zd168* mutant lineages produced extra SDQs. Loss of *cnt-2* also altered other asymmetric divisions that produce apoptotic cells (see Table S1 and Supplemental Results available online). Analyses of genetic interactions between *cnt-2* and either *pig-1* or *ham-1*, which is necessary for some of the asymmetric divisions that require *pig-1* and *cnt-2*, suggest that they could act in the same pathway (Table S2; Supplemental Results).

Loss of CNT-2 Affects Q.p Neuroblast Daughter Size

Q.p daughters differ in size, with Q.pp being smaller than its mitotic sister Q.pa [4, 8]. The wild-type precursor is approximately four times the size of its sister, whereas *cnt-2* Q.p daughters are equivalent in size (Figures 1D and 1E; Movie S1; Movie S2). We considered the possibility that apoptosis causes Q.pp to contract, resulting in the size asymmetry, but ruled out this possibility in two ways. First, we analyzed the sizes of the Q.p daughters in a *ced-4* mutant where Q.pp survives and found that Q.pa was still more than three times the size of its sister (Figure 1D). Second, we followed the Q.p division using time-lapse confocal microscopy. The wild-type cleavage furrow was displaced toward the posterior, resulting in different-sized daughter cells; the *cnt-2* mutant furrow formed in a central position (Figure 1E; Movie S1; Movie S2).

CNT-2 Arf GAP Activity Is Essential for Its Function

Of the three CNT-2 isoforms, B isoform expression with (CNT-2B::GFP) or without a GFP tag (CNT-2B) showed the most effective rescue of the extra A/PVM defect (Figure 2C; data not shown). To ask whether CNT-2 activity depends on a functional GAP domain, we changed a conserved arginine to lysine at position 709 [CNT-2B(RK)::GFP], which abrogates AGAP1's GAP activity while still allowing the cognate Arf to bind [9]. We also changed cysteine to serine at positions 681 and 684 [CNT-2B(CCSS)::GFP], which should render the Arf GAP incapable of binding its cognate Arf [9, 10]. Both changes abolished CNT-2B's rescuing activity (Figure 2C).

[4]Present address: Laboratory of Developmental Genetics, Rockefeller University, 1230 York Avenue, New York, NY 10065, USA

[5]Present address: Genentech, Inc., 1 DNA Way, MS37, South San Francisco, CA 94080, USA

[6]Present address: National Laboratory of Biomacromolecules, Institute of Biophysics, Chinese Academy of Sciences, 15 Datun Road, Chaoyang District, Beijing 100101, China

[7]Present address: Regeneron Pharmaceuticals, 777 Old Saw Mill River Road, Tarrytown, NY 10591, USA

[8]Present address: Biology Department, University of Nevada, Reno, NV 89557, USA

*Correspondence: garriga@berkeley.edu

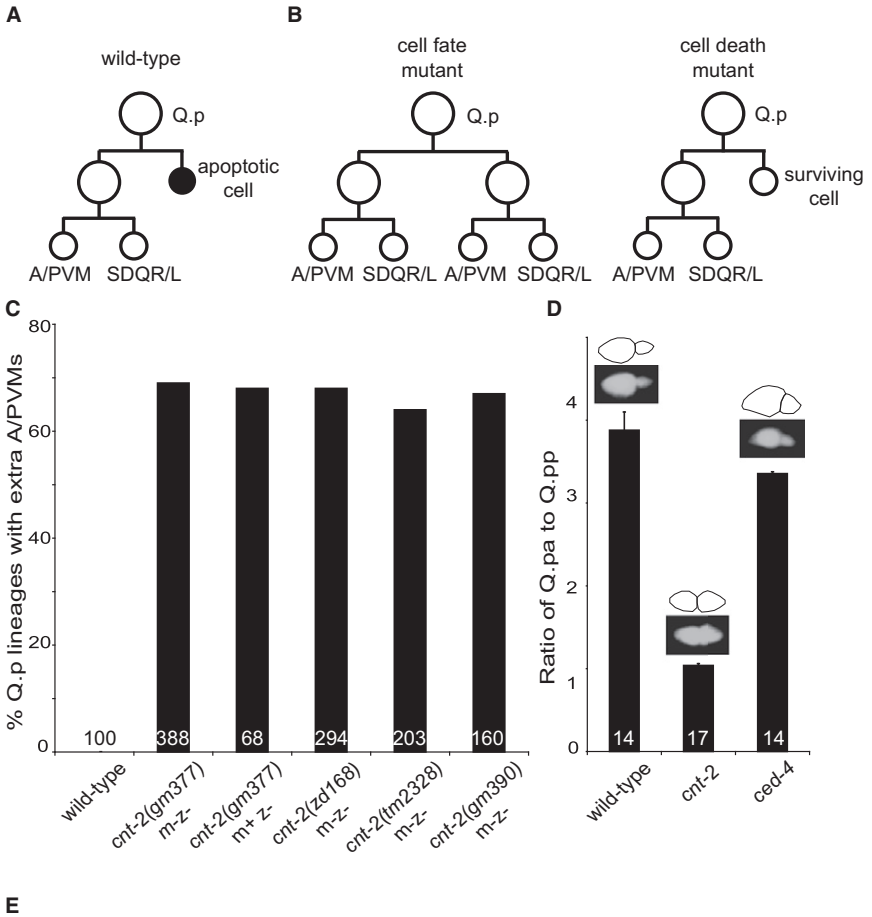

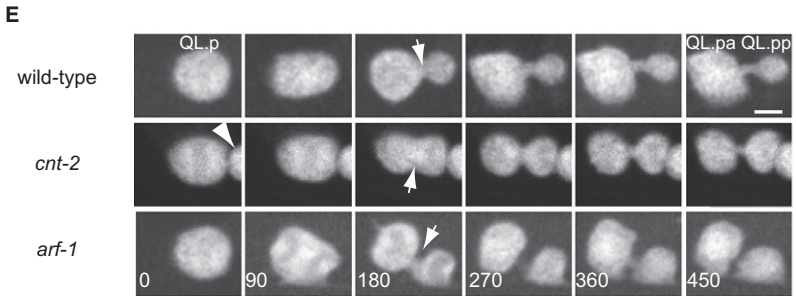

Figure 1. *cnt-2* Mutations Disrupt the Asymmetric Divisions of the Q.p Neuroblast

(A) The Q.p lineage.

(B) The Q.p lineage in cell fate (left) and cell death (right) mutant animals.

(C) Frequency of extra A/PVM neurons in *cnt-2* mutants. All of the animals carried the *Pmec-4::gfp* transgene *zdIs5*. *cnt-2* mutant lineages produced either a single A/PVM or two A/PVMs (% Q.p lineages with extra A/PVMs are shown). Animals were mutant for both maternal and zygotic *cnt-2* (m−z−) or only for zygotic *cnt-2* (m+z−). For this and subsequent graphs, the number of Q.p lineages scored is above each genotype.

(D and E) Alleles analyzed were *cnt-2(gm377)*, *ced-4(n1162)*, and *arf-1(ok796)*. Animals contained the *Pegl-17::gfp* transgene *ayIs9*.

(D) Ratio of the Q.p daughter cell sizes. Above the bars are representative photomicrographs and drawings of Q.p daughter cells. Error bars represent standard error of the mean.

(E) Fluorescence photomicrographs from time-lapse confocal recordings of wild-type, *cnt-2*, and *arf-1* Q.p divisions. See also Movie S1, Movie S2, and Movie S3. Numbers at the bottom left corner of each frame represents the time in seconds. Arrows indicate the position of the cleavage furrow. Normally, the QL.a cell migrates over the top of Q.p toward the tail and then divides. QL.ap, the PQR neuron, continues to migrate toward the tail, but QL.aa dies. The arrowhead indicates a QL.aa cell that did not die. Scale bar represents 2 μm.

We also asked whether excess CNT-2 caused an A/PVM phenotype. Expression of full-length wild-type or mutant CNT-2 did not (Figure 2C), but expression of the N-terminal deletion mutant ΔNCNT-2::GFP, which lacks the GLD, produced animals with extra A/PVMs (Figure 2D) and Q.p daughters that were more equivalent in size (Figure 3A). Mutations in proapoptotic genes enhance the A/PVM defect of *pig-1* mutants or animals treated with *cnt-2* RNA interference (RNAi) [4, 11, 12] (data not shown), and a *ced-4* mutation enhanced the A/PVM phenotype caused by ΔNCNT-2::GFP (Figure 2D). The requirement for Arf GAP activity (Figure 2D), however, suggests that ΔNCNT-2::GFP does not act as a dominant negative. Moreover, the ability of ΔNCNT-2::GFP expression to partially rescue the A/PVM phenotype of *cnt-2* mutants shows that the transgenic protein has normal CNT-2 activity (Figure 2D). Experiments presented below support the hypothesis that ΔNCNT-2::GFP possesses deregulated Arf GAP activity.

CNT-2 Functions Cell Autonomously

CNT-2 could regulate either secretion of a signal to Q.p or a membrane trafficking event in Q.p. To determine where CNT-2 acts, we expressed *cnt-2B* from the *mab-5* promoter. *mab-5* encodes a transcription factor expressed in cells near the tail [13, 14]. With the exception of Q descendents, bilaterally symmetric cells express *mab-5* on both the left and right. The left Q.p, which generates PVM, but not the right Q.p, which generates AVM, expresses *mab-5* [15]. If *cnt-2* acts in the Q lineage, its expression from the *mab-5* promoter should rescue the PVM but not the AVM defect of *cnt-2* mutants. If *cnt-2* acts in cells that signal to Q.p, its expression from the *mab-5* promoter should either rescue or fail to rescue both the PVM and AVM defects, depending on whether CNT-2 acts in *mab-5*-expressing cells. Consistent with CNT-2 acting in the Q lineage, *cnt-2B* expression from the *mab-5* promoter rescued the PVM but not the AVM defects (Figure 3B). We also placed the *Pmab-5::cnt-2B* transgene into a *cnt-2; egl-20* mutant background. Transcription of *mab-5* in the QL lineage but not in other cells requires the Wnt EGL-20 [16]. Loss of *egl-20* abolished the ability of the *Pmab-5::cnt-2* transgene to rescue the PVM defect of the *cnt-2* mutant, consistent with CNT-2 acting in the Q lineage (data not shown).

CNT-2 Functions in Endocytosis

To address how CNT-2 regulates trafficking, we asked whether *cnt-2* mutants exhibited defects in receptor-mediated

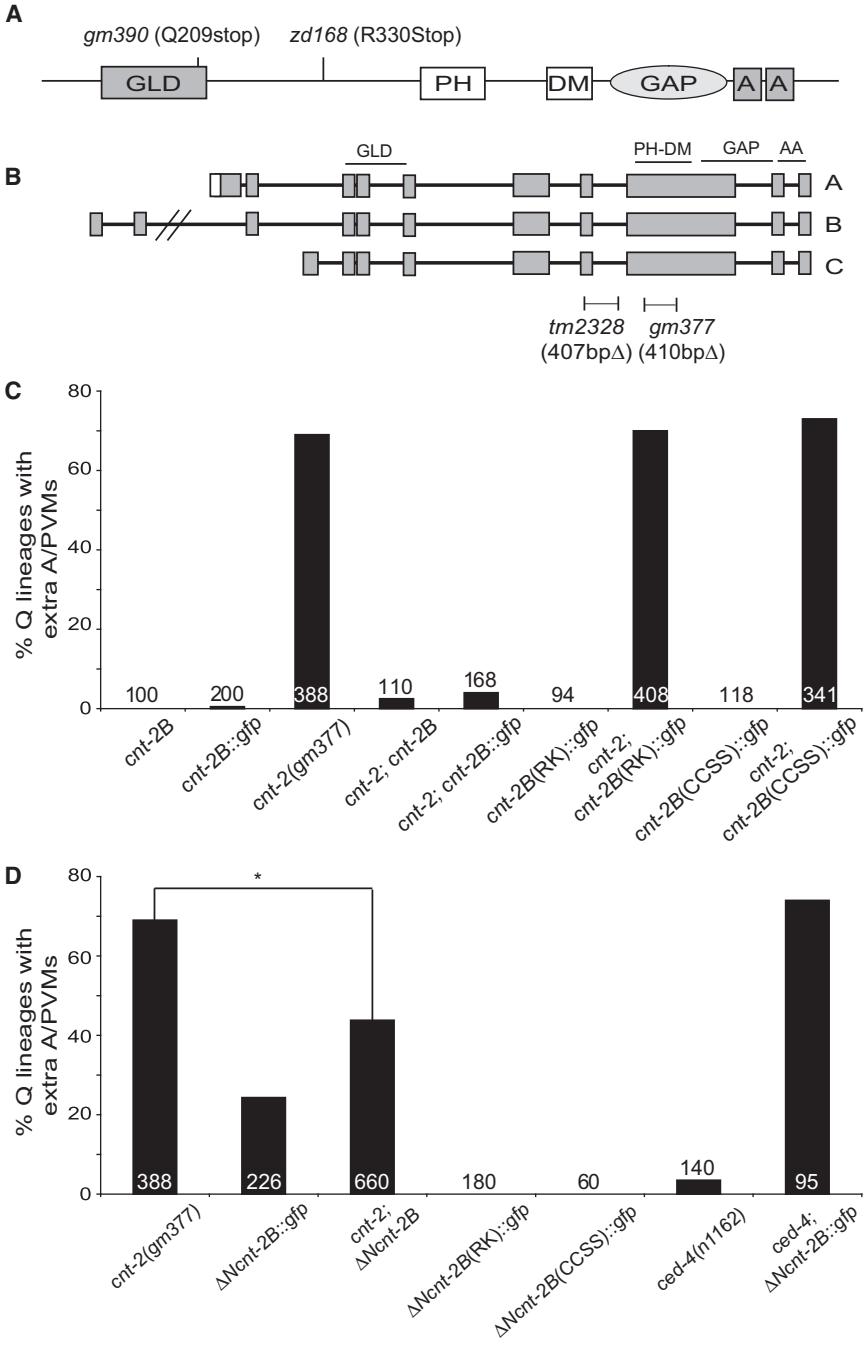

Figure 2. CNT-2 and the Role of Its GAP Domain in the Q.p Division

(A) Structure of CNT-2B. The following abbreviations are used: GLD, GTPase-like domain; PH and DM, split pleckstrin homology domain; GAP, Arf GTPase-activating protein domain; A, ankyrin repeats.

(B) Structure of the A, B, and C mRNAs. Boxes represent exons; lines represent introns. Shaded boxes represent coding sequences; the open box represents the 5′ untranslated region of isoform A. The slashes in intron 1 of isoform B indicate that the intron length is larger than drawn. The *tm2328* and *gm377* deletions are predicted to shift the reading frame.

(C and D) Effects of *cnt-2* transgenes on the Q.p lineage. Data are presented as in Figure 1C. The mutation that changes a conserved arginine to lysine at position 709 [CNT-2B(RK)::GFP] abrogated the GAP activity of AGAP1 while still allowing the cognate Arf to bind [9]. The cysteine-to-serine changes at positions 681 and 684 within the zinc-finger motif [CNT-2-2B(CCSS):: GFP] are predicted to render the Arf GAP incapable of binding its cognate Arf [9, 10]. We generated one transgenic line for *cnt-2B*, five for *cnt-2B::gfp*, two each for the mutated versions of *cnt-2B::gfp* and Δ*Ncnt-2B::gfp*, and three for Δ*Ncnt-2B::gfp*. Each of the lines for a particular construct was tested and gave similar results. Data for only one line of each type are presented. GFP levels were similar for all of the transgenes. *p < 0.0001 (two-sample proportion test).

endocytosis [17]. The intestine secretes vitellogenins, which are internalized by the RME-2 receptor on mature oocytes. Endocytosis-defective oocytes fail to internalize vitellogenins, resulting in their accumulation in the pseudocoelom and their absence from mature oocytes. Tagged vitellogenin VIT-2::GFP accumulated in the pseudocoelom of *cnt-2* mutants (data not shown). Compared to wild-type oocytes, fewer *cnt-2* oocytes contained VIT-2::GFP (Figures 4A and 4B).

Aberrant RME-2 trafficking can alter VIT-2::GFP distribution [18]. More RME-2::GFP accumulated at the cell surface of *cnt-2* oocytes than wild-type oocytes (Figures 4C–4E), and RME-2::GFP localized occasionally to juxtanuclear dots that were observed in endocytosis mutants (Figure 4D) [18]. Taken together, the VIT-2::GFP and RME-2::GFP phenotypes suggest that CNT-2 regulates endocytosis.

To test the hypothesis that compromised endocytosis contributes to the *cnt-2* asymmetric division phenotypes, we asked whether reducing the levels of endocytosis molecules by RNAi affected the Q.p division. We used an *rrf-3* mutant background to sensitize the animals to the effects of RNAi [19], and a weak *ced-3(n2436)* mutation. RNAi of endocytosis genes resulted in lethality, but escapers of RNAi to *dyn-1*, which encodes the dynamin homolog, or to *rab-5* resulted in significant numbers of extra A/PVMs ($p < 0.001$): 21% (n = 66) for *dyn-1* and 20% (n = 133) for *rab-5*. The negative control produced 7% extra A/PVMs (n = 197), and *cnt-2(RNAi)* produced 49% extra A/PVMs (n = 218). Rab5 homologs specifically mediate endocytic trafficking [20], supporting the hypothesis that CNT-2 regulates endocytic events that control the Q.p division.

The GTPase Genes *arf-1* and *arf-6* Regulate the Q.p Division

The essential role for the GAP domain of CNT-2 indicates that *arf*s or *arf-like* (*arl*) genes regulate the Q.p division. Sequence

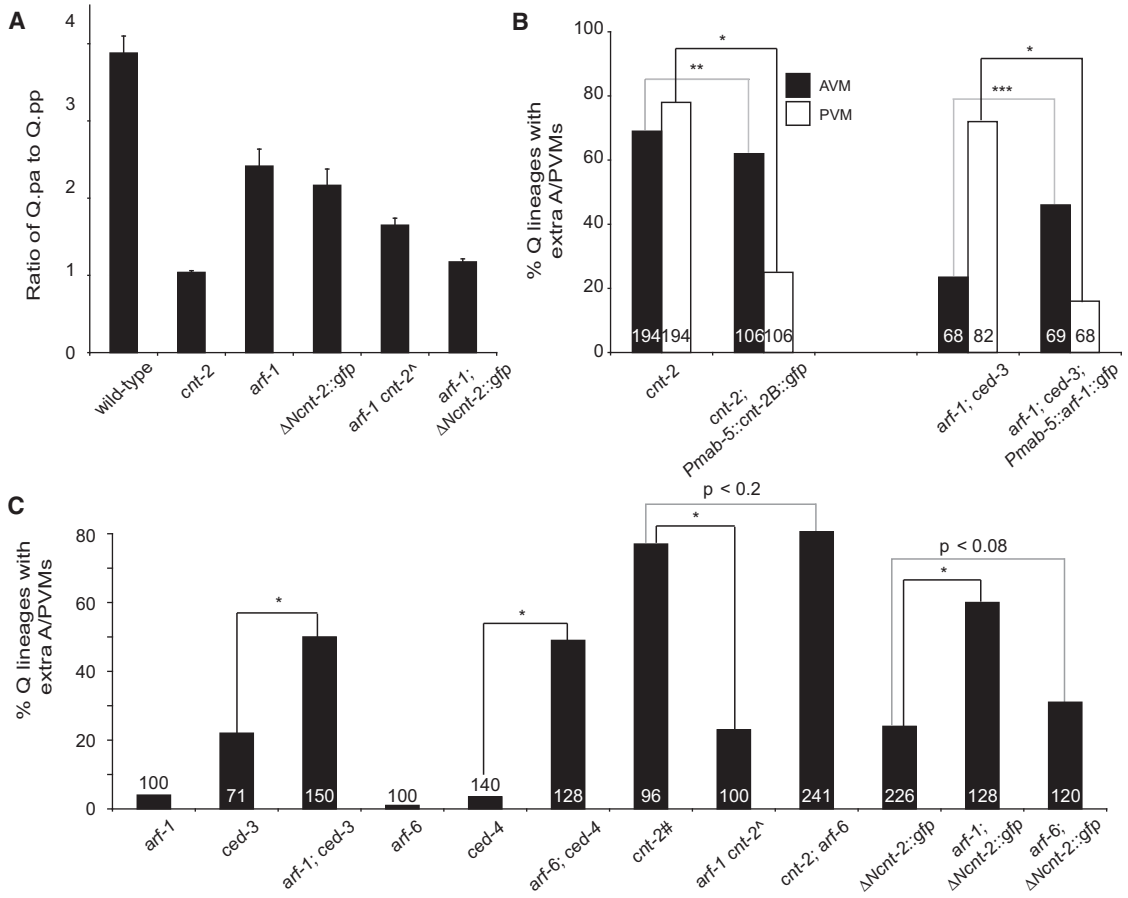

Figure 3. Cell-Autonomous Roles and Genetic Interactions for *arf-1* and *cnt-2*

Alleles used were *arf-1(ok796)*, *arf-6(tm1447)*, *ced-3(n717)*, *ced-4(n1162)*, and *cnt-2(gm377)*.

(A) Ratio of the Q.p daughter cell sizes. Data are presented as in Figure 1D. Error bars represent standard error of the mean.

(B) Expression of a *cnt-2* or an *arf-1* cDNA from the *mab-5* promoter rescued the QL (PVM) but not the QR (AVM) defects of *cnt-2* or *arf-1;ced-3* mutant animals, respectively. The frequency of extra AVMs (white bars) and PVMs (black bars) is presented separately. Data are presented as in Figure 1C.

(C) The roles of *arf-1* and *arf-6* in the Q.p division. Data are presented as in Figure 1C.

(A and C) Because *arf-1* and *cnt-2* are linked on *LG III*, *unc-32(e189)* and *dpy-18(e364)* are visible markers used to construct the *arf-1 cnt-2* double mutant. ∧The *arf-1 cnt-2* chromosome also contained an *unc-32* mutation. #The *cnt-2* control in (C) contained the *unc-32* and *dpy-18* mutations.

*p < 0.0001, **p < 0.3, ***p < 0.01.

analysis defines three Arf classes: class I (Arf1–3), class II (Arf4 and 5), and the more divergent class III (Arf6) [21]. *C. elegans* has a single representative of each class [22]. The *C. elegans* genome also encodes ten Arls.

Knocking down the function of each of the *arf* or *arl* homologs by RNAi in the *rrf-3; ced-3(n2436)* mutant background produced extra A/PVMs with *arf-1*, *arf-3*, and *arf-6* (S.C. and J.T., unpublished data). A single deletion allele of each *arf* gene exists. The *arf-3* mutants arrest as larvae and do not have an A/PVM phenotype, either alone or in a *ced-3* mutant background (data not shown). Off-target effects could explain the discrepancy between the RNAi and mutant phenotypes because *arf-3* is closely related to *arf-1*. Alternatively, maternal *arf-3* provided by the heterozygous mothers could mask a role for *arf-3* in the Q.p division. By contrast, *arf-1* and *arf-6* mutants displayed a weak extra A/PVM phenotype and enhanced the extra A/PVM phenotype of *ced-3* or *ced-4* mutants (Figure 3C). Because *arf-1* interacted genetically with *cnt-2* (see below), we addressed its role in the Q.p division, and we found that *arf-1* regulates Q.p daughter cell size (Figure 1E; Figure 3A; Movie S3) and acts autonomously in the Q lineage (Figure 3B).

arf-1 and *cnt-2* Genetic Interactions

The *arf-6* mutation failed to interact with either the *cnt-2* mutant or ΔNCNT-2::GFP (Figure 3C). Loss of *arf-1*, by contrast, suppressed the extra A/PVM and size asymmetry defects of *cnt-2* mutants (Figure 3A and 3C). Suppression of the extra A/PVM defect resulted from a failure of the A/PVMs to differentiate and express the GFP marker (Figure S1; Supplemental Results).

To address the possibility that CNT-2 is an ARF-1 GAP, we asked whether *arf-1* and *cnt-2* mutants have similar oocyte phenotypes. RNAi of *arf-1* disrupts VIT-2::GFP uptake into oocytes [17]. VIT-2::GFP accumulated in the pseudocoelom of the *arf-1* mutant, and fewer mutant oocytes contained VIT-2::GFP (Figures 4A and 4B; data not shown). We rarely detected RME-2::GFP in *arf-1* mutants, suggesting that it may not be trafficked to the plasma membrane (Figures 4C–4E).

Distinct RME-2::GFP phenotypes support a model where ARF-1 and CNT-2 act in antagonistic cycles. This model predicts that an *arf-1 cnt-2* double mutant should alter the RME-2::GFP phenotypes of the single mutants. As the model predicts, knocking down *cnt-2* resulted in *arf-1* oocytes with

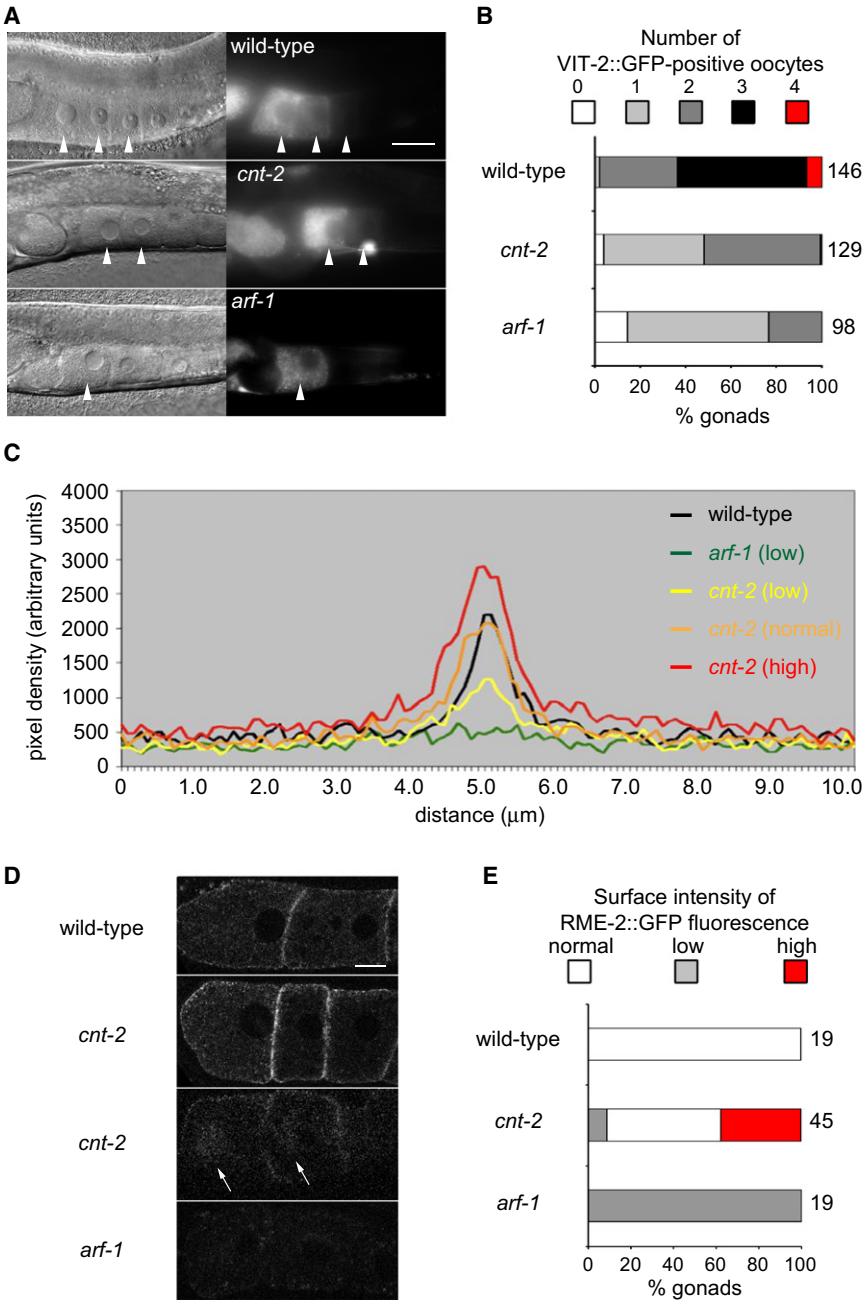

Figure 4. CNT-2 Regulates Receptor-Mediated Endocytosis

arf-1(ok796) and *cnt-2(gm377)* were used.

(A) Nomarski (left panels) and fluorescence photomicrographs (right panels) of wild-type, *cnt-2*, and *arf-1* animals containing *[vit-2::gfp]*. Arrowheads indicate the positions of individual oocytes. Scale bar represents 30 μm.

(B) Quantification of the number of VIT-2::GFP-positive oocytes in a gonad arm. To the right of the bars are the numbers of gonad arms scored. $p < 0.0001$ for both *arf-1* and *cnt-2* compared to wild-type using a two-sample test for proportions.

(C) Plots of line scans through the first two oocytes of wild-type, *arf-1*, and *cnt-2* mutants that contain the *rme-2::gfp* transgene. ImageJ was used to draw a line perpendicular to, and centered on, the boundary between the first and the second oocyte on 12-bit depth confocal images. The plot profile for this line was recorded, and five independent profiles were averaged for each gonad. Based on the maximum intensity of fluorescence (Imax) measured in arbitrary units (AU), gonads were grouped into low (Imax < 1000 AU), normal (1000 AU < Imax < 2500 AU), or high (Imax > 2500 AU) fluorescence classes. The three classes of RME-2::GFP surface intensity quantified in (E) are depicted here. The range of the normal class is illustrated by the wild-type and *cnt-2* scans.

(D) Confocal imaging of RME-2::GFP in wild-type and mutant oocytes. Arrows indicate juxtanuclear dots. Scale bar represents 10 μm.

(E) Quantification of RME-2::GFP levels at the oocyte cell surface. $p < 0.0001$ for both *arf-1* and *cnt-2* compared to wild-type using a two-sample test for proportions. The number of oocytes scored is to the right of each bar. Figure S2 describes the effects of interactions between *arf-1* and *cnt-2* on RME-2::GFP distribution.

more RME-2::GFP at the cell surface (Figure S2; Supplemental Results).

The *arf-1* mutation also interacted genetically with ΔNCNT-2::GFP, enhancing the daughter cell size and extra A/PVM phenotypes (Figures 3A and 3C). The opposite effects of *arf-1* loss on *cnt-2* mutants and transgenic animals confirm that ΔNCNT-2::GFP does not simply interfere with *cnt-2* function. We propose that the GLD of CNT-2 negatively regulates CNT-2 function. Deregulated GAP activity of ΔNCNT-2::GFP might enhance endocytosis, leading to an asymmetric cell division defect. Excessive or decreased endocytosis might disrupt Q.p asymmetry. Alternatively, the N terminus of CNT-2 might restrict its activity to a particular membrane compartment, the ΔNCNT-2::GFP phenotype resulting from CNT-2 acting in an inappropriate trafficking event.

The requirement for CNT-2 GAP function argues that Arfs or Arls regulate the Q.p division. Why then were we unable to identify a cognate GTPase? Eliminating CNT-2 or its cognate GTPase should disrupt a specific membrane trafficking step and result in a similar phenotype. If this assumption is correct, one explanation for the discrepancy is that CNT-2 regulates ARF-3 but that the contribution of maternal *arf-3* masked its role in mutant animals. Alternatively, CNT-2 could regulate more than one GTPase. Elimination of two or more GTPases would generate a phenotype similar to that of *cnt-2* mutants. The GTPases could provide overlapping functions in the same trafficking event or could mediate distinct events. Consistent with the latter possibility, the two mammalian CNT-2 homologs interact with different adaptors that mediate distinct trafficking events [23]. As the sole *C. elegans* AGAP, CNT-2 could mediate both events. This model is consistent with the mixed-oocyte phenotype of *cnt-2* mutants: some oocytes accumulate excess cell surface RME-2::GFP, revealing an endocytosis defect, whereas other oocytes have low RME-2::GFP levels, revealing a distinct defect.

Membrane Trafficking and Development

Trafficking of membrane receptors plays important roles in developmental decisions. Defects in Notch trafficking can lead to inappropriate activation of the receptor [24]. Components of the trafficking machinery can also exhibit specificity for particular cargo. Neural tube closure requires specific interactions between the Van Gogh homolog Vangl2 and the sec24b subunit of the COPII complex to transport Vangl2 from the endoplasmic reticulum to the Golgi [25]. Whether CNT-2 exhibits specificity for particular cargo is unclear. Notch and Wnt signaling regulate asymmetric cell divisions in *Drosophila* and *C. elegans*, respectively [26, 27]. The involvement of these molecules in asymmetric cell divisions raises the interesting possibility that CNT-2 regulates Notch or Wnt pathways.

Experimental Procedures

C. elegans genetics and DNA manipulations are described in the Supplemental Experimental Procedures.

Lineage Analysis

Animals were maintained at 22°C. L1 larvae were anesthetized with 0.1% levamisole in M9 buffer and mounted on 2% agar pads. Images were acquired on a Zeiss Axiovert 200M microscope with a 100× 1.45 NA oil objective and an electron-multiplying charge-coupled C9100-13 device camera (Hamamatsu Photonics) using the 488 nm line of a CSU10 argon laser attached to a spinning-disk confocal scan head (Yokogawa; obtained from Solamere, Inc.). Images were acquired every 90 s using μManager software (www.micro-manager.org).

Oocyte Endocytosis and Q.p Daughter Sizes

L4 larvae were collected and observed as young adults 24 hr later. Fluorescence images of *bIs1[vit-2::GFP]* gonads were obtained with a Zeiss Axioskop 2 microscope. Images were collected using an ORCA-ER CCD camera (Hamamatsu Photonics) and Openlab imaging software (Improvision). Confocal sections of *pwIs116[rme-2::RME-2-GFP]* oocytes were obtained with a Zeiss LSM 510 confocal microscope equipped with a 100× 1.3 NA oil objective and the 488 nm line of an LGK 7812 ML4 argon laser (LASOS Lasertechnik). 1024 × 1024 single monodirectional line scans were performed at medial positions of gonads to obtain 12-bit images for light-intensity measurements.

For Q.p daughter cell sizes, QL.pa and QL.pp cell areas were measured in L1 larvae that had their left sides up. Areas were measured in triplicate using ImageJ. The size ratio was calculated using average area values. QL.pa and QL.pp were imaged only when the Q.pp did not appear apoptotic, was not rounded, and was still attached to Q.pa.

Supplemental Information

Supplemental Information includes Supplemental Results, two figures, two tables, Supplemental Experimental Procedures, and three movies and can be found with this article online at doi:10.1016/j.cub.2011.04.025.

Acknowledgments

We thank Yuji Kohara for providing *cnt-2* cDNAs, Shohei Mitani and the National BioResource Project for providing the *cnt-2(tm2328)* mutant, and Nancy Hawkins for providing unpublished data. Some nematode strains used in this work were provided by the Caenorhabditis Genetics Center, which is funded by the National Institutes of Health (NIH) National Center for Research Resources (NCRR). This work was supported by NIH grants NS39397 to S.G.C. and NS42213 to G.G. R.D.V. was supported by the Howard Hughes Medical Institute and NIH grant R37GM38499 G.O. was supported by a fellowship from the Damon Runyon Cancer Research Foundation, and J.T. was supported by a fellowship from the Association pour la Recherche sur le Cancer.

Received: July 6, 2010
Revised: March 21, 2011
Accepted: April 13, 2011
Published online: May 19, 2011

References

1. Sulston, J.E., and Horvitz, H.R. (1977). Post-embryonic cell lineages of the nematode, Caenorhabditis elegans. Dev. Biol. *56*, 110–156.
2. Sulston, J.E., Schierenberg, E., White, J.G., and Thomson, J.N. (1983). The embryonic cell lineage of the nematode Caenorhabditis elegans. Dev. Biol. *100*, 64–119.
3. Singhvi, A., and Garriga, G. (2009). Asymmetric divisions, aggresomes and apoptosis. Trends Cell Biol. *19*, 1–7.
4. Cordes, S., Frank, C.A., and Garriga, G. (2006). The C. elegans MELK ortholog PIG-1 regulates cell size asymmetry and daughter cell fate in asymmetric neuroblast divisions. Development *133*, 2747–2756.
5. Ellis, H.M., and Horvitz, H.R. (1986). Genetic control of programmed cell death in the nematode C. elegans. Cell *44*, 817–829.
6. Kahn, R.A., Bruford, E., Inoue, H., Logsdon, J.M., Jr., Nie, Z., Premont, R.T., Randazzo, P.A., Satake, M., Theibert, A.B., Zapp, M.L., and Cassel, D. (2008). Consensus nomenclature for the human ArfGAP domain-containing proteins. J. Cell Biol. *182*, 1039–1044.
7. Randazzo, P.A., and Hirsch, D.S. (2004). Arf GAPs: Multifunctional proteins that regulate membrane traffic and actin remodelling. Cell. Signal. *16*, 401–413.
8. Ou, G., Stuurman, N., D'Ambrosio, M., and Vale, R.D. (2010). Polarized myosin produces unequal-size daughters during asymmetric cell division. Science *330*, 677–680.
9. Nie, Z., Stanley, K.T., Stauffer, S., Jacques, K.M., Hirsch, D.S., Takei, J., and Randazzo, P.A. (2002). AGAP1, an endosome-associated, phosphoinositide-dependent ADP-ribosylation factor GTPase-activating protein that affects actin cytoskeleton. J. Biol. Chem. *277*, 48965–48975.
10. Cukierman, E., Huber, I., Rotman, M., and Cassel, D. (1995). The ARF1 GTPase-activating protein: Zinc finger motif and Golgi complex localization. Science *270*, 1999–2002.
11. Frank, C.A., Hawkins, N.C., Guenther, C., Horvitz, H.R., and Garriga, G. (2005). C. elegans HAM-1 positions the cleavage plane and regulates apoptosis in asymmetric neuroblast divisions. Dev. Biol. *284*, 301–310.
12. Guenther, C., and Garriga, G. (1996). Asymmetric distribution of the C. elegans HAM-1 protein in neuroblasts enables daughter cells to adopt distinct fates. Development *122*, 3509–3518.
13. Costa, M., Weir, M., Coulson, A., Sulston, J., and Kenyon, C. (1988). Posterior pattern formation in C. elegans involves position-specific expression of a gene containing a homeobox. Cell *55*, 747–756.
14. Cowing, D.W., and Kenyon, C. (1992). Expression of the homeotic gene mab-5 during Caenorhabditis elegans embryogenesis. Development *116*, 481–490.
15. Salser, S.J., and Kenyon, C. (1992). Activation of a C. elegans Antennapedia homologue in migrating cells controls their direction of migration. Nature *355*, 255–258.
16. Maloof, J.N., Whangbo, J., Harris, J.M., Jongeward, G.D., and Kenyon, C. (1999). A Wnt signaling pathway controls hox gene expression and neuroblast migration in C. elegans. Development *126*, 37–49.
17. Grant, B., and Hirsh, D. (1999). Receptor-mediated endocytosis in the Caenorhabditis elegans oocyte. Mol. Biol. Cell *10*, 4311–4326.
18. Balklava, Z., Pant, S., Fares, H., and Grant, B.D. (2007). Genome-wide analysis identifies a general requirement for polarity proteins in endocytic traffic. Nat. Cell Biol. *9*, 1066–1073.
19. Simmer, F., Tijsterman, M., Parrish, S., Koushika, S.P., Nonet, M.L., Fire, A., Ahringer, J., and Plasterk, R.H. (2002). Loss of the putative RNA-directed RNA polymerase RRF-3 makes C. elegans hypersensitive to RNAi. Curr. Biol. *12*, 1317–1319.
20. Zerial, M., and McBride, H. (2001). Rab proteins as membrane organizers. Nat. Rev. Mol. Cell Biol. *2*, 107–117.
21. Kahn, R.A., Cherfils, J., Elias, M., Lovering, R.C., Munro, S., and Schurmann, A. (2006). Nomenclature for the human Arf family of GTP-binding proteins: ARF, ARL, and SAR proteins. J. Cell Biol. *172*, 645–650.
22. Li, Y., Kelly, W.G., Logsdon, J.M., Jr., Schurko, A.M., Harfe, B.D., Hill-Harfe, K.L., and Kahn, R.A. (2004). Functional genomic analysis of the ADP-ribosylation factor family of GTPases: Phylogeny among diverse eukaryotes and function in C. elegans. FASEB J. *18*, 1834–1850.
23. Nie, Z., Fei, J., Premont, R.T., and Randazzo, P.A. (2005). The Arf GAPs AGAP1 and AGAP2 distinguish between the adaptor protein complexes AP-1 and AP-3. J. Cell Sci. *118*, 3555–3566.
24. Fortini, M.E., and Bilder, D. (2009). Endocytic regulation of Notch signaling. Curr. Opin. Genet. Dev. *19*, 323–328.

25. Merte, J., Jensen, D., Wright, K., Sarsfield, S., Wang, Y., Schekman, R., and Ginty, D.D. (2010). Sec24b selectively sorts Vangl2 to regulate planar cell polarity during neural tube closure. Nat. Cell Biol. *12*, 41–46, 1–8.
26. Doe, C.Q., and Spana, E.P. (1995). A collection of cortical crescents: Asymmetric protein localization in CNS precursor cells. Neuron *15*, 991–995.
27. Mizumoto, K., and Sawa, H. (2007). Two betas or not two betas: Regulation of asymmetric division by beta-catenin. Trends Cell Biol. *17*, 465–473.